



Journal of Applied Sciences

ISSN 1812-5654

science
alert

ANSI*net*
an open access publisher
<http://ansinet.com>

Adaptive Control of a Double-Electromagnet Suspension System

¹R. Barzamini, ²A.R. Yazdizadeh, ¹H.A. Talebi and ¹H. Eliasi

¹Faculty of Electrical Engineering, Amirkabir University of Technology, Tehran, Iran

²Faculty of Electrical Engineering, Power and Water University of Technology, Tehran, Iran

Abstract: In this study, an adaptive controller is presented that addresses the coupling effects between two groups of electromagnetic trains. The main application of DEM (Double Electro-Magnet) is rapid rail transportation. Since the number of passengers are stochastic, the mass of the train will be variable too. On the other hand, due to the variation of the DEM parameters (such as coil inductance) in a real environment, the system is to be controlled in a proper manner. The proposed method in this study overcomes all of these problems. The module, based on some reasonable assumptions of nonlinear mathematical model, is modeled as a double-electromagnet system. The proposed algorithm has a satisfying performance in tracking in presence of unknown changes in the mass. The advantage of the proposed algorithm in comparison to non-linear controllers is that knowing the mass changes is not necessary. It is also important to make sure that a control system is robust against measurement noises, because all sensors collect noise from the environment. Due to the presence of input and output perturbation, the new proposed algorithm shows satisfying performance. The results show that the proposed method is less sensitive to perturbation in the input.

Key words: Double-electromagnet, model reference adaptive control, suspension, nonlinear, feedback linearization

INTRODUCTION

Today, express trains have significantly eased traffic congestions in urban areas. The basic idea in designing such trains is the magnetic suspension. As shown in Fig. 1, in a single suspension system, the mass is under the influence of two forces: the force of gravity and the magnetic force. In the case of passenger trains, a different type of suspension system as shown in Fig. 2 is used.

In fact, the two groups of electromagnets embedded in a module are connected with a rigid body: therefore their motion states are coupled. Currently, the general control method controls the two groups of electromagnets separately using two independent controllers, each of which acts according to respective controlled object: the coupling between the two groups of electromagnets is regarded as disturbance and suppressed by enhancing the robustness of individual controllers. However, this method cannot actively overcome the uncertainty issues and the control performance is not desirable especially in the presence of external disturbances.

In recent years so many studies have been carried out on electromagnet suspension systems. Chen *et al.* (2003) presented a larger moving range dual-axis magnetic-levitation (maglev) system. A repulsive maglev system with four active guiding tracks was adopted. The

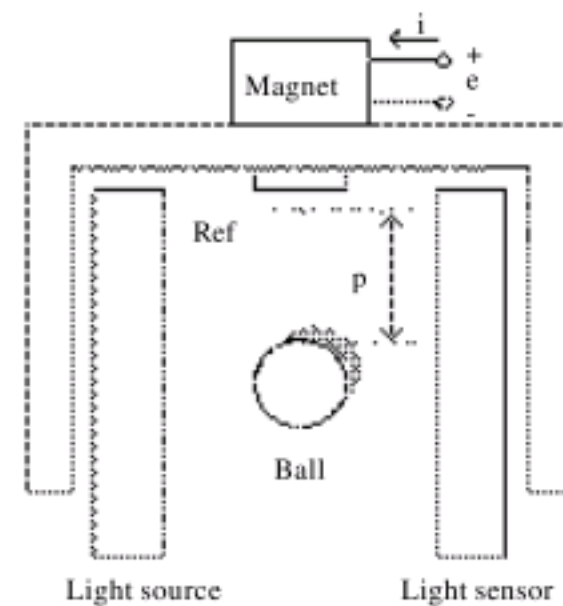


Fig. 1: Magnetic suspension system

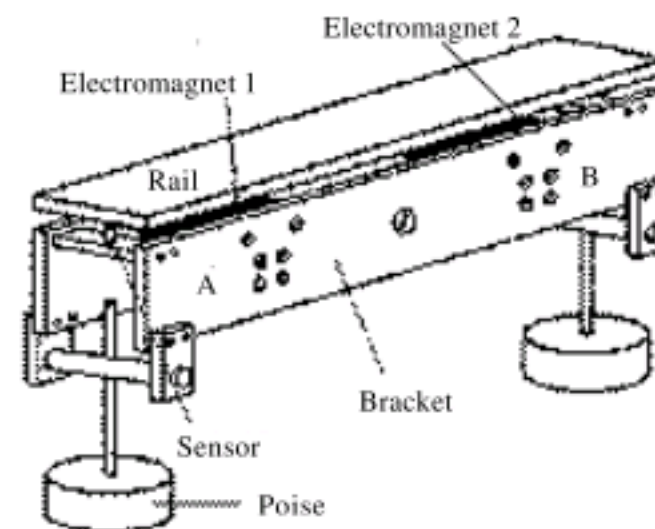


Fig. 2: The structure of the suspension system

system was treated as a multi-input multi-output system and an adaptive controller was designed. Huang and Lin (2003) proposed a novel adaptive fuzzy sliding mode controller and successfully employed it to control an active hydraulic suspension system. A maglev transportation system including levitation and propulsion control is the subject of considerable scientific interest because of highly nonlinear and unstable behaviors. Wai and Lee (2008a), based on the concepts of mechanical geometry and motion dynamics, developed the dynamic model of a maglev transportation system including levitated electromagnets and a propulsive Linear Induction Motor (LIM). Then, a model-based Sliding Mode Control (SMC) strategy was introduced. Moreover, Wai and Lee (2008b) focused on the sequential developments of backstepping-based control systems including a Backstepping Control (BSC), an adaptive BSC (ABSC) and an adaptive dynamic surface control (ADSC) for the levitated positioning of the linear maglev rail system. Yang *et al.* (2008) proposed an adaptive robust output feedback controller for the position tracking problem of a magnetic levitation system while using a noisy position sensor. Bonivento *et al.* (2005) addressed the problem of positioning a ball in a vertical magnetic field created by a pair of electromagnets while rejecting some external disturbances. The presence of uncertainties on the physical parameters characterizing the system has been taken into account, designing a control law capable of solving the problem robustly. De Queiroz and Pradhananga (2007) presented a general formulation for constructing stabilizing control laws with a time-varying bias flux. The design of a bias flux function of the mechanical states, general conditions were established on the bias function that ensures a singularity-free controller and power losses that converge to zero as the mechanical states converge to zero, without affecting the system stability. Position regulation of a magnetic levitation device is achieved through a Control Lyapunov Function (CLF) feedback design. Peterson *et al.* (2006) showed experimentally that, by selecting the CLF based on the solution to an algebraic Riccati equation, it is possible to tune the performance of the controller using intuition from classical LQR control. Lin *et al.* (2005) proposed a hybrid controller using a Recurrent Neural Network (RNN) to control a levitated object in a magnetic levitation system. A nonlinear dynamic model of the system is described and a computed force controller, based on feedback linearization, is proposed, based on feedback linearization, to control the position of the levitated object. Fialho and Balas (2002) presented a framework for designing road adaptive suspension controllers. Linear parameter-varying techniques were used in combination

with nonlinear backstepping to achieve the desired nonlinear response of the vehicle suspension. Hasanzadeh *et al.* (2008) defined an objective function based (on) transient response of step response. Then considered a maglev system as a case study in which by using genetic algorithm, the optimal controller parameters could be assigned. Aliasghary *et al.* (2008) introduced classical and hybrid methods for controlling the Maglev system. A new RBF-sliding mode control method, a new FEL-sliding mode control for Maglev were proposed, which combines the merits of adaptive neural network and sliding mode control.

The goal of designing an adaptive controller for a double magnetic suspension system is to suspend an object in a certain distance from a magnetic rail by using two electromagnets. As mentioned before, one of the most significant applications of magnetic suspension is in express trains. The advantage of the suggested method over the work done by De-Sheng *et al.* (2006) is that their presented decoupled controller shows no robustness to mass changes, parameters changes, noise and outer disturbance; so that for example, with a small variation into the train, the performance of their proposed method will decrease. However the current study will solve the mentioned problems and improves their method.

MATERIALS AND METHODS

Double Electro-Magnet (DEM) has five degrees of freedom in movements: heave, sway, pitch, roll and yaw; Among them, only heave and pitch movements are to be controlled: hence the system in this case has two degrees of freedom.

Variable parameters: The in hand variable parameters in the problem are: the mass of the object (m) and the inductance of the coil of the electromagnets (K).

System modeling: Structure of the system: The structure of DEM shown in Fig. 2 includes two identical electromagnets which are connected by a rigid bracket. Magnets 1 and 2 provide the suspension forces needed for points 1 and 2, respectively. The suspended object can be considered as a solid object with two electromagnets. In addition, two sensors are used to measure the states of the suspension and two poises can be used to provide load forces.

Double Electro-Magnet can be simplified as shown Fig. 3. Parameters of the system are defined as follows: m is the mass of the suspended object, I is the spinning inertia in the center of the object O , F_1 and F_2 are magnetic forces, N_1 and N_2 are load forces on the two ends of the

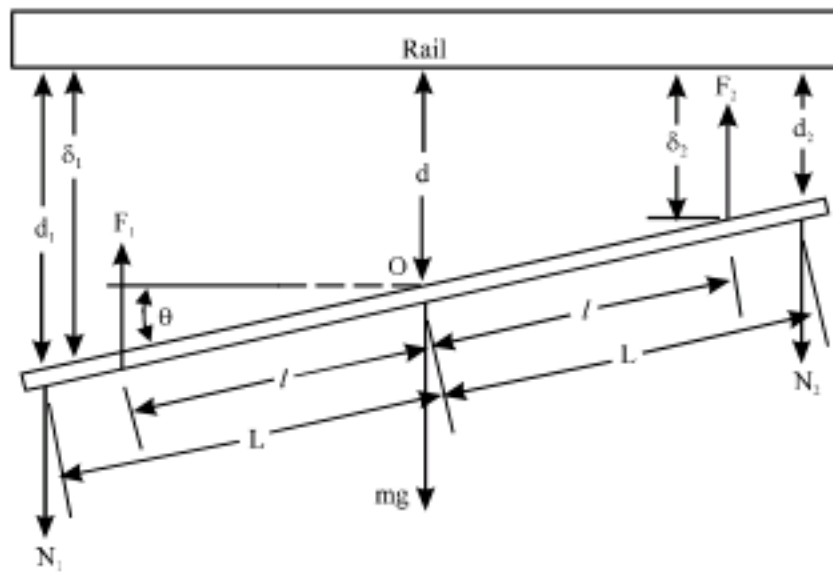


Fig. 3: Details of suspension system

bracket, d is the distance of the center of the object from the rail, δ_1 and δ_2 are the distances from the points where, F_1 and F_2 are applied, respectively. d_1 and d_2 are the distances between the solid object and the corresponding points on the rail. l is the distance between the center of the object O and the point where magnetic forces are applied and finally, L is the distance between the center of the object and the point where load forces are applied.

Simplifying assumptions

- The stiffness of the rail is assumed to be infinite and only the movement of the DEM relative to the rail is significant
- It is assumed that leakage flux, edge effect of the magnetic force, magnetic resistance of the core and the rail are negligible
- A weight center is considered for the weight of the object. The weight of the two magnets is assumed to be identical: therefore, the total weight of the bracket and the magnets can be represented by a weight center, O , shown in Fig. 3
- The lengths of the magnets are assumed to be very small and the points where the forces are applied are fixed
- Load forces, created by the poises, have only one downward component

Double Electro-Magnet (DEM) suspension system is a complex system including mechanical dynamics of DEM, the relation between the current and the electromagnetic force and the relation between the voltage and the current.

Mechanical- dynamic equations: Double Electro-Magnet (DEM) has five degrees of movement freedom: heave, sway, pitch, roll and yaw. For the controller, only heave

and pitch movements are taken into account. Vertical movement and the movements of the weight center, O and the twisting are movements around the main rotation pivot. The positive directions of movement and rotation are downward and counter-clockwise, respectively. According to the principle of force transfer and the second law of Newton, the mechanical dynamics equations are obtained as follows:

$$m\ddot{d} = -F_1 - F_2 + N_1 + N_2 + mg \tag{1a}$$

$$I\ddot{\theta} = N_1L - N_2L - F_1l + F_2l \tag{1b}$$

According to Fig. 3, we have:

$$d = (d_1 + d_2)/2 \tag{2a}$$

$$\theta \approx (d_1 - d_2)/2L \tag{2b}$$

Using Eq. 1 and 2, we have:

$$\ddot{d}_1 = -A_k \times F_1 - B_k \times F_2 + C_k \times N_1 + D_k \times N_2 + g \tag{3a}$$

$$\ddot{d}_2 = -B_k \times F_1 - A_k \times F_2 + D_k \times N_1 + C_k \times N_2 + g \tag{3b}$$

where, the parameters are defined as:

$$A_k = \frac{1}{m} + \frac{Ll}{I} \tag{4a}$$

$$B_k = \frac{1}{m} - \frac{Ll}{I} \tag{4b}$$

$$C_k = \frac{1}{m} + \frac{L^2}{I} \tag{4c}$$

$$D_k = \frac{1}{m} - \frac{L^2}{I} \tag{4d}$$

Magnetic force equation: The magnetic force between the rail and the magnets can be represented as:

$$F = Ki^2 / \delta^2 \tag{5}$$

where, K is the inductance coefficient, δ is the distance between the rail and magnets and i is the electrical current of the coil of the magnet. According to Fig. 3 we have:

$$\delta_1 = d + \theta \times l = Pd_1 + Qd_2 \tag{6a}$$

$$\delta_2 = d - \theta \times l = Qd_1 + Pd_2 \tag{6b}$$

Where:

$$P = (L+l)/(2L) \tag{7a}$$

$$Q = (L-l)/(2L) \tag{7b}$$

Hence, the magnetic force in Fig. 3 can be represented as follows:

$$F_1 = K \frac{i_1^2}{\delta_1^2} = K \frac{i_1^2}{(Pd_1 + Qd_2)^2} \tag{8a}$$

$$F_2 = K \frac{i_2^2}{\delta_2^2} = K \frac{i_2^2}{(Qd_1 + Pd_2)^2} \tag{8b}$$

Electrical-dynamic equations: The electrical-dynamic equations of the electro-magnetic suspension system can be considered as a resistance-inductance circuit and this can be modeled as follows:

$$u(t) = Ri + \frac{2Ki}{\delta} - \frac{2Ki\dot{\delta}}{\delta^2} \tag{9}$$

where, u (t) is the control voltage of the magnet and R is the total resistance of the whole circuit. Using Eq. 5-7, we have the electrical equations of the magnet 2 as follows:

$$u_1(t) = Ri_1 + \frac{2Ki_1}{(Pd_1 + Qd_2)} - \frac{2Ki_1(\dot{Pd}_1 + Q\dot{d}_2)}{(Pd_1 + Qd_2)^2} \tag{10a}$$

$$u_2(t) = Ri_2 + \frac{2Ki_2}{(Qd_1 + Pd_2)} - \frac{2Ki_2(Q\dot{d}_1 + \dot{Pd}_2)}{(Qd_1 + Pd_2)^2} \tag{10b}$$

where, u₁(t) and u₂(t) are the control voltages of the two magnets.

The state space representation: Let us select the state of the system as follows:

$$x = [x_1, x_2, x_3, x_4, x_5, x_6]^T \\ = [d_1, \dot{d}_1, d_2, \dot{d}_2, i_1, i_2]^T \tag{10}$$

The one may come up with the following equations as the state-space representation of the system:

$$\dot{x} = f(x) + G(x)u \\ y = h(x) \tag{11}$$

Where:

$$f(x) = \begin{bmatrix} x_2 \\ \frac{-A_K Kx_5^2}{(Px_1 + Qx_3)^2} + \frac{-B_K Kx_6^2}{(Qx_1 + Px_3)^2} + C_K \times N_1 + D_K \times N_2 + g \\ x_4 \\ \frac{-B_K Kx_5^2}{(Px_1 + Qx_3)^2} + \frac{-A_K Kx_6^2}{(Qx_1 + Px_3)^2} + D_K \times N_1 + C_K \times N_2 + g \\ -\frac{R}{2K} x_5 (Px_1 + Qx_3) + \frac{x_5 (Px_2 + Qx_4)}{(Px_1 + Qx_3)} \\ -\frac{R}{2K} x_6 (Qx_1 + Px_3) + \frac{x_6 (Qx_2 + Px_4)}{(Qx_1 + Px_3)} \end{bmatrix} \tag{12}$$

$$G(x) = \begin{bmatrix} 0 & 0 \\ 0 & 0 \\ 0 & 0 \\ 0 & 0 \\ \frac{(Px_1 + Qx_2)}{2K} & 0 \\ 0 & \frac{(Qx_1 + Px_2)}{2K} \end{bmatrix} \tag{13}$$

$$h(x) = \begin{bmatrix} h_1(x) \\ h_2(x) \end{bmatrix} = \begin{bmatrix} x_1 \\ x_3 \end{bmatrix}$$

In the following the case where all system parameters are not exactly known is to be investigated.

The case in which the exact values of some parameters of the system are not known is to be investigated. It is inevitable to apply adaptive methods for controlling such systems. Designing an adaptive controller includes two major steps:

- The control law
- The adaptation law

In this study a linearizing feedback is proposed. The introduced feedback is very useful in designing the control law.

ADAPTIVE CONTROL

Assume the nonlinear system can be represented as the following companion form,

$$y^{(n)} + \sum_{i=1}^n \alpha_i f_i(x) = bu \tag{14}$$

Then designing the control law and the adaptation law can be done by using the exact feedback linearization: the dynamic equation of the system can be expressed as:

$$\ddot{y} = L_f^2 h + L_g L_f h \times u \tag{15}$$

In case where all system parameters are known, the control law is given by:

$$u = \frac{1}{L_g L_f^2 h} (-L_f^3 h + v) \tag{16}$$

However, in this study it is assumed that the parameters of the system are not exactly known. Hence the exact values of the functions $L_f^3 h$ and $L_g L_f^2 h$ are not known either and therefore, the Eq. 16 cannot be realized to obtain the control law. In this study, the idea of substituting the parameters by their estimation is introduced, which lead us to the following control law (Khalil, 2002):

$$u = \frac{1}{(L_g L_f^2 h)_e} (- (L_f^3 h)_e + v) \tag{17}$$

Now, the necessary conditions for implementation of this method should be discussed: The first step is to represent the functions $f(x)$ and $g(x)$ linear in parameters. Hence, the coefficients are considered as some unknown parameters that are to be estimated. Hence, the estimated values of $L_f^3 h$ and $L_g L_f^2 h$ can be obtained and an adaptation law for the estimation of coefficients can be presented. The second step is to find an estimate for each $L_f^i h$, $i = 1, \dots, n-1$, which is the derivative of the output.

Suppose that $f(x)$ and $g(x)$ are linear in parameters (as will be shown, this is possible for the discussed system):

$$f(x) = \sum_{i=1}^{n1} \alpha_i f_i(x), \quad g(x) = \sum_{i=1}^{n2} \beta_i g_i(x) \tag{18}$$

where, f_i and g_i are some known functions and α_i and β_i are unknown parameters that are to be estimated. Now, by considering the discussed form for $f(x)$ and $g(x)$, an expression for $L_f^i h$, $L_g L_f^{i-1} h$, $i = 1, 2, \dots, r$ should be found. Where, r is the system relative degree.

$$L_f^i h = \sum_{j1=1}^{n1} \sum_{j2=1}^{n1} \dots \sum_{j_i=1}^{n1} L_{f_{j1}} (L_{f_{j2}} \dots (L_{f_{j_i}} h)) \alpha_{j1} \alpha_{j2} \dots \alpha_{j_i}, \quad i = 1, \dots, r \tag{19}$$

$$L_g L_f^{i-1} h = \sum_{k=1}^{n2} \sum_{j1=1}^{n1} \dots \sum_{j_{i-1}=1}^{n1} L_{g_k} (L_{f_{j1}} \dots (L_{f_{j_{i-1}}} h)) \beta_k \alpha_{j1} \dots \alpha_{j_{i-1}}$$

Having the equations, some new unknown above parameters emerge which are the combinations of previous unknown parameters. By estimating the new unknown parameters, the estimated values of $L_f^i h$, $L_g L_f^{i-1} h$, $i = 1, 2, \dots, r$ can be obtained. Now, we return to the case in which the exact parameter values are known. It was mentioned that for such cases the control

parameter v is chosen as follows so the trace error converges to zero.

$$v = y_d^{(r)} - k_{r-1} e^{(r-1)} - \dots - k_0 e, \quad e = y - y_d \tag{20}$$

We use the derivatives of the output which are not available. Hence their estimates are used. In such case, the estimated value of v is defined as follows:

$$v_e = y_d^{(r)} - k_{r-1} (L_f^{r-1} h)_e - \dots - k_0 e, \quad e = y - y_d \tag{21}$$

It is known that the relative degree of the system is three. Hence, the control law is given by:

$$u = \frac{1}{(L_g L_f^2 h)_e} (- (L_f^3 h)_e + v_e) \tag{22}$$

Now, it is time to discuss the necessary adaptation law for determining the values of the unknown parameters. In order to do so, first the control input defined in Eq. 21 is substituted in Eq. 16, hence we have:

$$\ddot{y} = L_f^3 h + \frac{L_g L_f^2 h}{(L_g L_f^2 h)_e} (- (L_f^3 h)_e + v_e) \tag{23}$$

Subtracting v from the above equation results in:

$$\ddot{e} + k_1 \dot{e} + k_2 e + k_3 e = L_f^3 h + \frac{L_g L_f^2 h}{(L_g L_f^2 h)_e} (- (L_f^3 h)_e + v_e) - v \tag{24}$$

which can be written as:

$$\ddot{e} + k_1 \dot{e} + k_2 e + k_3 e = (L_f^3 h - (L_f^3 h)_e) + (L_g L_f^2 h - (L_g L_f^2 h)_e) \frac{(- (L_f^3 h)_e + v_e)}{(L_g L_f^2 h)_e} + v_e - v \tag{25}$$

Substituting the functions in Eq. 25 with their estimates in Eq. 19, the right hand side of the above equation can be written in standard regressor form.

$$\ddot{e} + k_1 \dot{e} + k_2 e + k_3 e = W^T \Phi \tag{26}$$

where, Φ is the difference between estimated ($\Phi = \theta_e - \theta$), W is the so-called nonlinear regressor.

This represents a relation between the tracking error and the estimations error of the parameters which can be written as:

$$(s^3 + k_1 s^2 + k_2 s + k_3) e = W^T \Phi \tag{27}$$

Now, we have:

$$e = \frac{1}{s^3 + k_1s^2 + k_2s + k_3} W^T \Phi = F(s)W^T \Phi \quad (28)$$

The transfer function $F(s)$ is not an SPR transfer function: therefore, it should be converted to a SPR transfer function by defining a new filtered error variable as (Slotine and Li, 1991):

$$e_1 = (s^2 + p_1s + p_2)e \quad (29)$$

where, the values of the coefficients p_1 and p_2 are found such that $(s^2 + p_1s + p_2)/(s^3 + k_1s^2 + k_2s + k_3)$ is an SPR transfer function. However, in order to obtain the adaptation law, the value of e_1 is needed which in turn requires the first and the second order derivatives of the tracking error (e). If direct differentiation is used to get these derivatives, the system becomes noise-sensitive: therefore this method is not applicable.

To obtain the adaptation law, first, a combination is defined as the error:

$$e_1 = e + [F(s)W^T \times \theta_e - F(s)(W^T \theta_e)] \quad (30)$$

Since, the constant coefficients are not affected by the filter $F(s)$, the above equation can be written as:

$$e_1 = e + [F(s)W^T \times \Phi - F(s)(W^T \Phi)] \quad (31)$$

Now, by using Eq. 27 and Eq. 31, we have:

$$e_1 = F(s)W^T \times \Phi \quad (32)$$

where, the variable ξ is defined as:

$$\xi^T = F(s)W^T \quad (33)$$

Now, by using Eq. 32 and 33, the adaptation law can be obtained by using either a gradient algorithm or a least square algorithm. In case of SISO system, the adaptation law obtained by the normalized least square algorithm is:

$$\dot{\theta}_e = \dot{\Phi} = \frac{-p\xi e_1}{1 + \xi^T p \xi} \quad (34a)$$

$$\dot{p} = \frac{p\xi\xi^T p}{1 + \xi^T p \xi} \quad (34b)$$

For the Multi Input Multi Output (MIMO) system ξ has a matrix form and the above equation changes to:

$$\begin{aligned} \dot{\theta}_e = \dot{\Phi} &= \frac{-p\xi e_1}{1 + \xi^T p \xi} \\ \dot{p} &= \frac{p\xi\xi^T p}{1 + \xi^T p \xi} \end{aligned} \quad (35)$$

The problem that may raise here is that the term $\xi^T p \xi$ may be very large and therefore $\dot{\theta}_e$ and \dot{p} become singular-like point and cause the parameters to diverge. To solve this issue, the adaptation law should be modified as follows:

$$\dot{\theta}_e = \dot{\Phi} = \frac{-p\xi e_1}{1 + \text{norm}(\xi^T p \xi)} \quad (36a)$$

$$\dot{p} = \frac{p\xi\xi^T p}{1 + \text{norm}(\xi^T p \xi)} \quad (36b)$$

This can be considered as a new variation of the normalized least square algorithm.

Implementation of the proposed model: In present case , $f(x)$ and $g(x)$ can be written as:

$$f(x) = -A_K K \begin{bmatrix} 0 \\ x_5^2 \\ \frac{(Px_1 + Qx_3)^2}{x_5^2} \\ 0 \\ x_6^2 \\ \frac{(Qx_1 + Px_3)^2}{x_6^2} \\ 0 \\ 0 \end{bmatrix} - B_K K \begin{bmatrix} 0 \\ x_6^2 \\ \frac{(Qx_1 + Px_3)^2}{x_6^2} \\ 0 \\ x_5^2 \\ \frac{(Px_1 + Qx_3)^2}{x_5^2} \\ 0 \\ 0 \end{bmatrix} \quad (37)$$

$$-\frac{R}{2K} \begin{bmatrix} 0 \\ 0 \\ 0 \\ 0 \\ x_5(Px_1 + Qx_3) \\ x_6(Qx_1 + Px_3) \end{bmatrix} + C_K \begin{bmatrix} 0 \\ N_1 \\ 0 \\ N_2 \\ 0 \\ 0 \end{bmatrix} + D_K \begin{bmatrix} 0 \\ N_2 \\ 0 \\ N_1 \\ 0 \\ 0 \end{bmatrix} + \begin{bmatrix} x_2 \\ g \\ x_4 \\ g \\ \frac{x_5(Px_2 + Qx_4)}{(Px_1 + Qx_3)} \\ \frac{x_6(Qx_2 + Px_4)}{(Qx_1 + Px_3)} \end{bmatrix}$$

$$G(x) = \frac{1}{2K} \begin{bmatrix} 0 & 0 \\ 0 & 0 \\ 0 & 0 \\ 0 & 0 \\ (Px_1 + Qx_2) & 0 \\ 0 & (Qx_1 + Px_2) \end{bmatrix} \quad (38)$$

According to Eq. 18 and 38, we have $n_1 = 6$ and $n_2 = 1$. Now, the derivatives of the output can be calculated as follows:

$$L_r h = \sum_{i=1}^6 \alpha_i^{(1)} L_{ri} h, L_{ri} = 0, i = 1, \dots, 5, L_{r6} h = \begin{bmatrix} x_2 \\ x_4 \end{bmatrix} \quad (39)$$

Hence:

$$L_r h = L_{r6} h = \begin{bmatrix} x_2 \\ x_4 \end{bmatrix} \quad (40)$$

$$L_r^2 h = \sum_{i=1}^6 \sum_{j=1}^6 \alpha_i \alpha_j L_{ri} (L_{rj} h) = \sum_{i=1}^6 \alpha_i L_{ri} (L_{r6} h),$$

$$L_{r1}(L_{r6} h) = \begin{bmatrix} \frac{x_5^2}{(Px_1 + Qx_3)^2} \\ \frac{x_6^2}{(Qx_1 + Px_3)^2} \end{bmatrix}, L_{r2}(L_{r6} h) = \begin{bmatrix} \frac{x_6^2}{(Qx_1 + Px_3)^2} \\ \frac{x_5^2}{(Px_1 + Qx_3)^2} \end{bmatrix}, \quad (41)$$

$$L_{r3}(L_{r6} h) = \begin{bmatrix} 0 \\ 0 \end{bmatrix}, L_{r4}(L_{r6} h) = \begin{bmatrix} N_1 \\ N_2 \end{bmatrix}, L_{r5}(L_{r6} h) = \begin{bmatrix} N_2 \\ N_1 \end{bmatrix},$$

$$L_{r6}(L_{r6} h) = \begin{bmatrix} g \\ g \end{bmatrix}$$

And finally $L_r^3 h$ can be expressed as:

$$L_r^3 h = \sum_{i=1}^6 \sum_{j=1}^6 \sum_{k=1}^6 \alpha_i \alpha_j \alpha_k L_{ri} (L_{rj} (L_{rk} h))$$

$$= \sum_{i=1}^6 \sum_{j=1}^6 \alpha_i \alpha_j L_{ri} (L_{rj} (L_{r6} h)),$$

$$L_{ri} (L_{rj} (L_{r6} h)) = 0, i = 1, \dots, 6, j = 3, \dots, 6$$

$$L_{rk} (L_{rj} (L_{r6} h)) = 0, j = 1, 2, k = 1, 2, 4, 5$$

$$L_{r3}(L_{r1}(L_{r6} h)) = \begin{bmatrix} \frac{2x_5^2}{(Px_1 + Qx_3)} \\ \frac{2x_6^2}{(Qx_1 + Px_3)} \end{bmatrix},$$

$$L_{r3}(L_{r2}(L_{r6} h)) = \begin{bmatrix} \frac{2x_6^2}{(Qx_1 + Px_3)} \\ \frac{2x_5^2}{(Px_1 + Qx_3)} \end{bmatrix},$$

$$L_{r6}(L_{r1}(L_{r6} h)) = \nabla_x (L_{r1}(L_{r6} h)) \times f_6, \quad (42)$$

$$L_{r6}(L_{r2}(L_{r6} h)) = \nabla_x (L_{r2}(L_{r6} h)) \times f_6,$$

As can be seen from the above equation, the function $L_r^3 h$ has four terms. The function $L_g L_r^2 h$ can be obtained in a similar way:

$$L_g L_r^2 h = \sum_{i=1}^6 \sum_{j=1}^6 \beta \alpha_i \alpha_j L_{gi} (L_{rj} (L_{r6} h))$$

$$= \sum_{i=1}^6 \beta \alpha_i L_{gi} (L_{r6} h) \quad (43)$$

$$L_{gi} (L_{r6} h) = 0, i = 3, \dots, 6$$

$$L_{g1}(L_{r6} h) = \nabla_x (L_{r1}(L_{r6} h)) \times G,$$

$$L_{g2}(L_{r6} h) = \nabla_x (L_{r2}(L_{r6} h)) \times G$$

To obtain the matrixes W and Φ , one can use Eq. 25. According to Eq. 38 and 41 we have:

$$\Phi = [\theta_1 \theta_2 \theta_3 \theta_4 \theta_5 \theta_6 \theta_7 \theta_8]^T -$$

$$\begin{bmatrix} \frac{A_k R}{2} & -A_k K & \frac{B_k R}{2} & -B_k K & -\frac{A_k}{2} & -\frac{B_k}{2} & C_k & D_k \end{bmatrix}^T \quad (44)$$

and

$$W = \begin{bmatrix} w_1^T \\ [\nabla_x (L_{r1} L_{r6} h) \times f_6 + k_1 (L_{r1} L_{r6} h)]^T \\ w_3^T \\ [\nabla_x (L_{r2} L_{r6} h) \times f_6 + k_1 (L_{r2} L_{r6} h)]^T \\ \nabla_x (L_{r1} L_{r6} h) \times G \times \frac{-(L_r^3 h)_c + v_c}{(L_g L_r^2 h)_c} \\ \nabla_x (L_{r2} L_{r6} h) \times G \times \frac{-(L_r^3 h)_c + v_c}{(L_g L_r^2 h)_c} \\ [k_1 (L_{r4} L_{r6} h)]^T \\ [k_1 (L_{r5} L_{r6} h)]^T \end{bmatrix} \quad (45)$$

In Eq. 45, k_1 is the coefficient of the dynamic of the error. Here, for the parameters to converge to their true values, matrix W must satisfy Persistently Excitation (PE) condition. The continuous stimulation condition of the signal should be discussed for the matrix W . The adaptation algorithm is given by Eq. 25.

Present proposed method can now be shown in Table 1.

The proposed control method is simulated by using MATLAB software. It is worth noting that that the current system is a coupled 2-input-2output system. Here, it is assumed that some of the parameters of the system (m (the mass of the plate), R (the resistance of the coils)

Table 1: Summary of the proposed adaptive control method

	$f(x) = \sum_{i=1}^6 \alpha_i f_i(x), g(x) = \beta g(x)$
Model of the system	α_i and β are introduced in Eq. 45 and 36
Control law	$u = \frac{-(L_r^3 h)_c + v_c}{(L_g L_r^2 h)_c}$
Dynamic model of the error	$e = \frac{1}{s^3 + k_1 s^2 + k_2 s + k_3} W^T \Phi$ $= F(s) W^T \Phi$
Combined error	$e_c = e + [F(s) W^T \times \theta_c - F(s)(W^T \theta_c)]$
Modified adaptation law	$\dot{\theta}_c = \Phi = \frac{-p \xi e_c}{1 + \text{norm}(\xi^T p \xi)}$ $\dot{p} = \frac{p \xi \xi^T p}{1 + \text{norm}(\xi^T p \xi)}$

Table 2: Parameters of the system

L (m)	l (m)	m (kg)	I (kg×m ²)	N	N ₁ (N)	N ₂ (N)	δ ₀ (m)
0.3	0.168	14.852	0.5648	663	36.5	36.5	0.005

and K (the inductance coefficient of the coils)) are not known. Since the unknown parameters are combination of the above parameters, by assigning values to the parameters m, R and K, initial values for the parameters that should be estimated can be easily obtained. The point here is that in this case, initial values of m, R and K should be known: these initial values cannot be set to zero because by doing so, the convergence of the parameters are jeopardized. In simulation, an unknown limited poise is assumed to be placed on the plate and the performance of the proposed adaptation algorithm is evaluated. It is noticeable that the value of \dot{y} is estimated in every time step. The initial values for m, R and K are 10, 15 and 0.1, respectively. The values of the Parameters are shown in Table 2.

The reference model: For the suspended plate to have a smooth motion, a reference model is used to provide the plate with appropriate motion conditions. The point is that the relative degree of the reference model should be greater or equal to the relative degree of the system. Since the relative degree of the system is equal to 3, the reference model is assumed as:

$$M(s) = \frac{0.25}{s^3 + 2s^2 + 1.25s + 0.25} \quad (46)$$

where, k_1 , k_2 and k_3 are 70, 1600 and 12000, respectively.

RESULTS AND DISCUSSION

The advantage of the proposed algorithm in comparison to non-linear controllers (De-Sheng *et al.*, 2006; Li and Chang, 1999; Liu *et al.*, 2005) is that knowing the mass changes is not necessary, it was also shown that in the presence of input and output perturbation, the modified proposed algorithm ends to the satisfying results (Namerikawa and Fujita, 2001).

In Fig. 4, the reference path that is to be followed is depicted. In addition, Fig. 5 shows the output of the system. As it can be shown, a smooth path for the motion of the plate is produced. In Fig. 6, the output of the system tracking the reference model path is shown: this figure shows the satisfactory performance of the control system tracking the desired path, but estimated parameters do not converge to the real values (Fig. 7, 8) because of the matrix W is not PE.

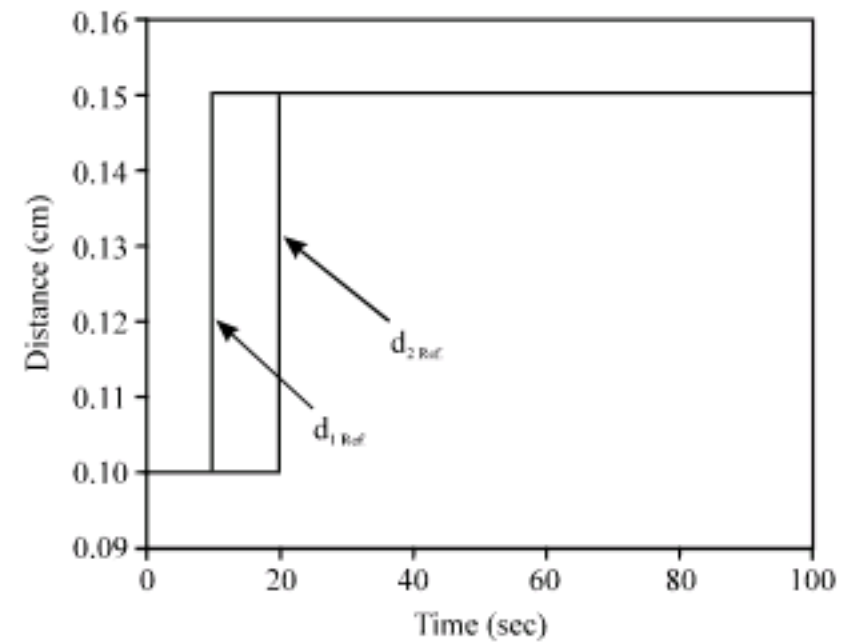


Fig. 4: The reference path

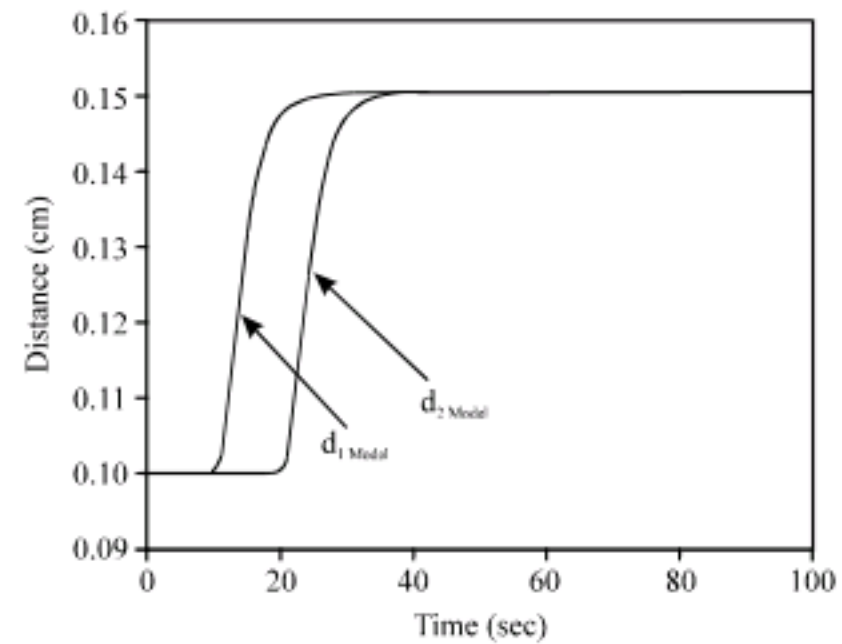


Fig. 5: The model output

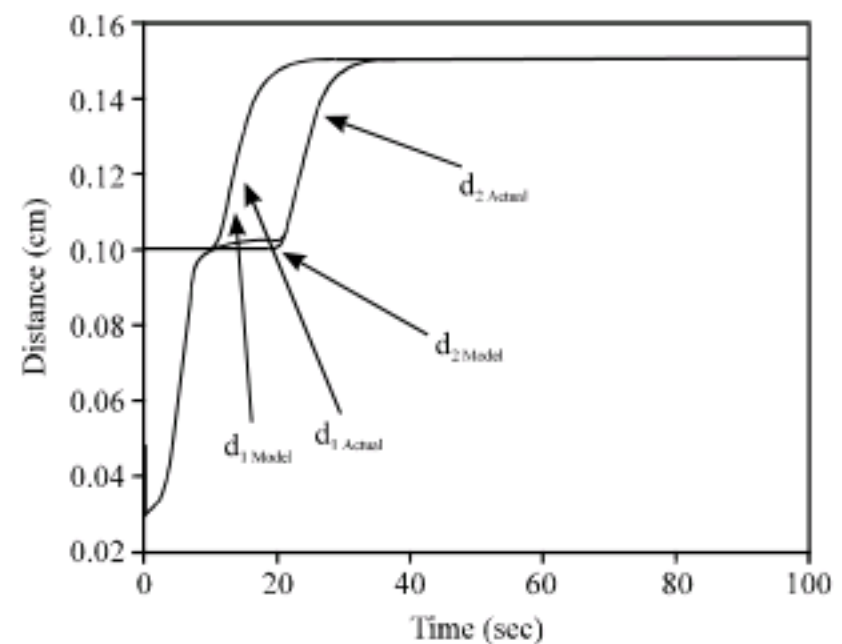


Fig. 6: Following the reference model path

Difficult paths are selected to show the abilities of the proposed control method in path following. In the path shown above, first one side of the plate approaches the reference value and then the other side does the same. Of course, such paths have the advantage of protecting the system from a sudden large amount of error.

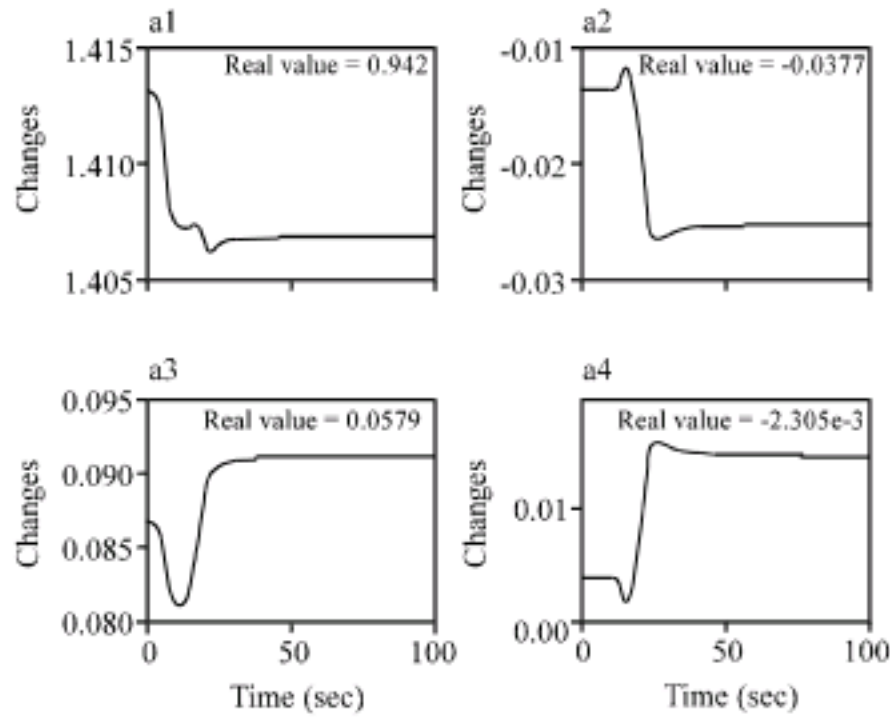


Fig. 7: Estimated parameters curves model path

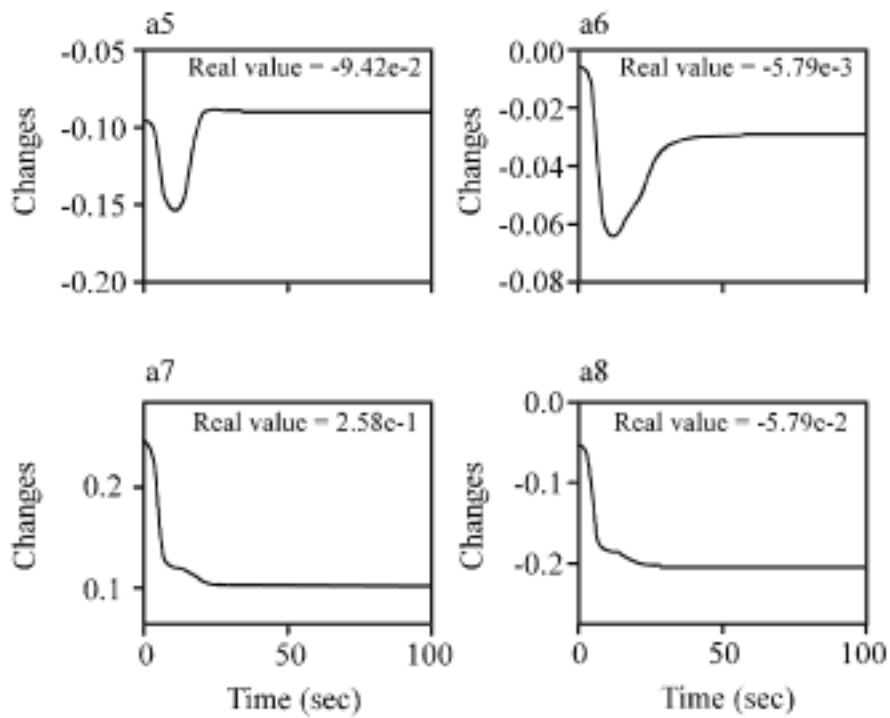


Fig. 8: Estimated parameters curves

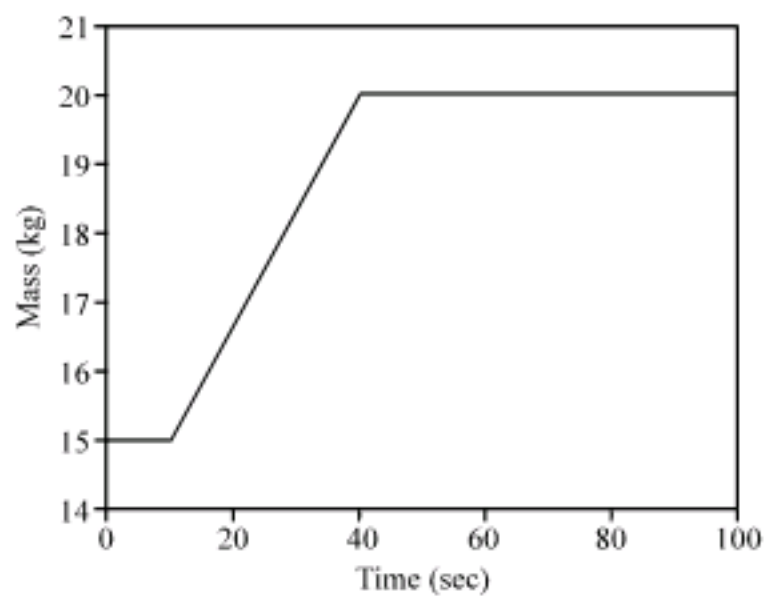


Fig. 9: Changes in the mass of the plate caused by the additional poises

For this part, the case in which the parameters of the system are not completely identified is studied and the performance of the controller is shown when an unknown poise is placed on the plate. Figure 9 shows the change in the mass of the plate caused by the additional poises.

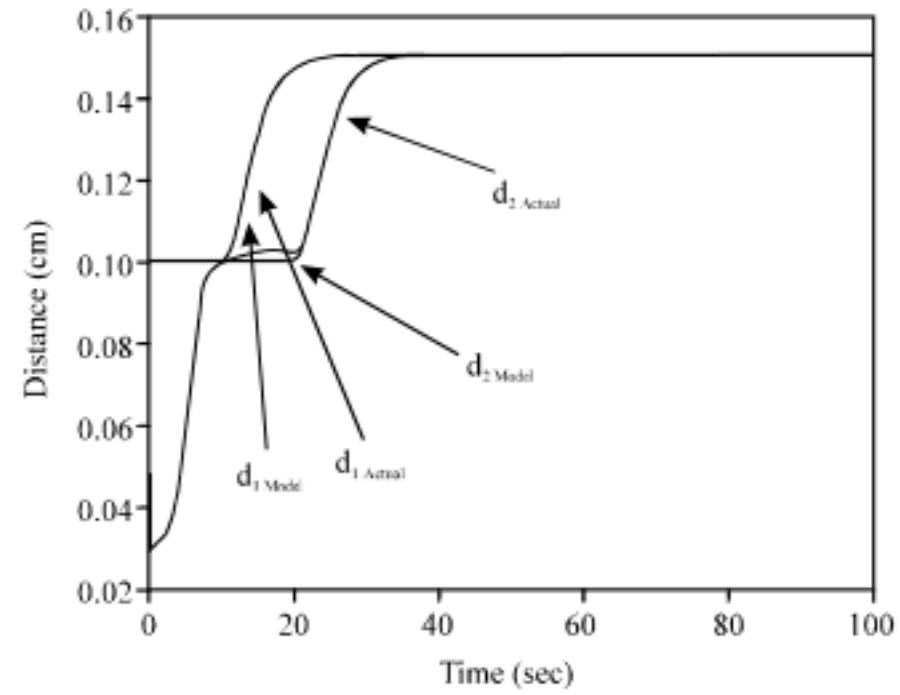


Fig. 10: Reference model path tracking in case of changes in the mass

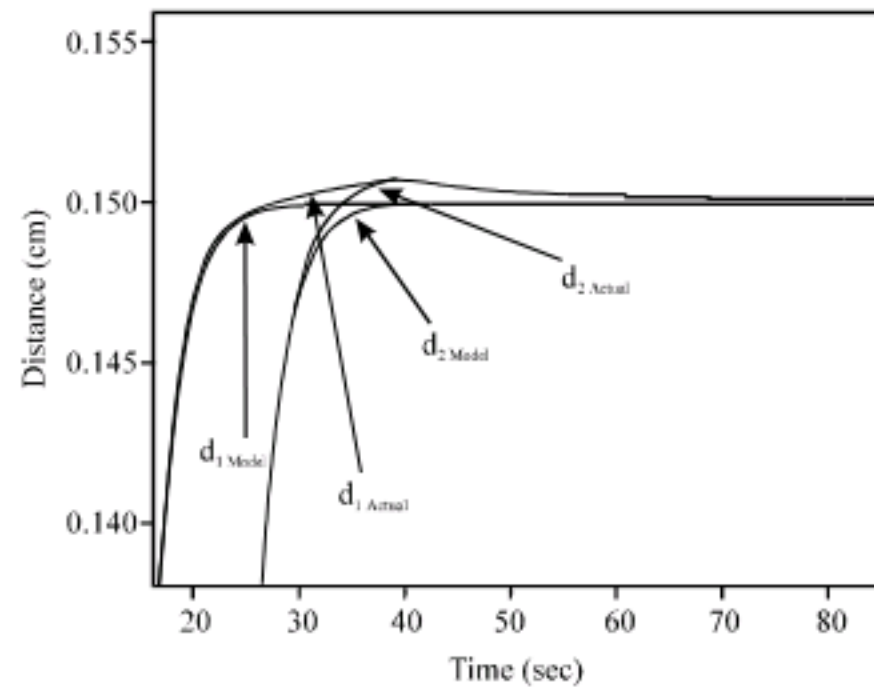


Fig. 11: The effects of the changes in mass on the output of the system

In Fig. 10, reference model path tracking, in the case of a changing mass for the plate, is depicted. As shown in Fig. 10, the proposed control algorithm is capable of producing a good control input for tracking of the reference model path. In order to visualize the effects of changes in mass on the output of the system, a part of Fig. 10 is magnified and shown in Fig. 11 and as can be shown, although the mass is changed, the tracking is well done. This is due to the effect of changes in mass that is compensated by the changes on the estimated parameters and the adaptation algorithm. The nature and the magnitude of the changes in mass should be known, otherwise a complete tracking would be impossible and the output of the system would have a steady state error. The proposed adaptive control method provides the capability of complete tracking with the mass changes being unknown.

In Fig. 11, the effect of the changes in mass is shown at 20th to 80th second time interval. Looking at Fig. 8, one

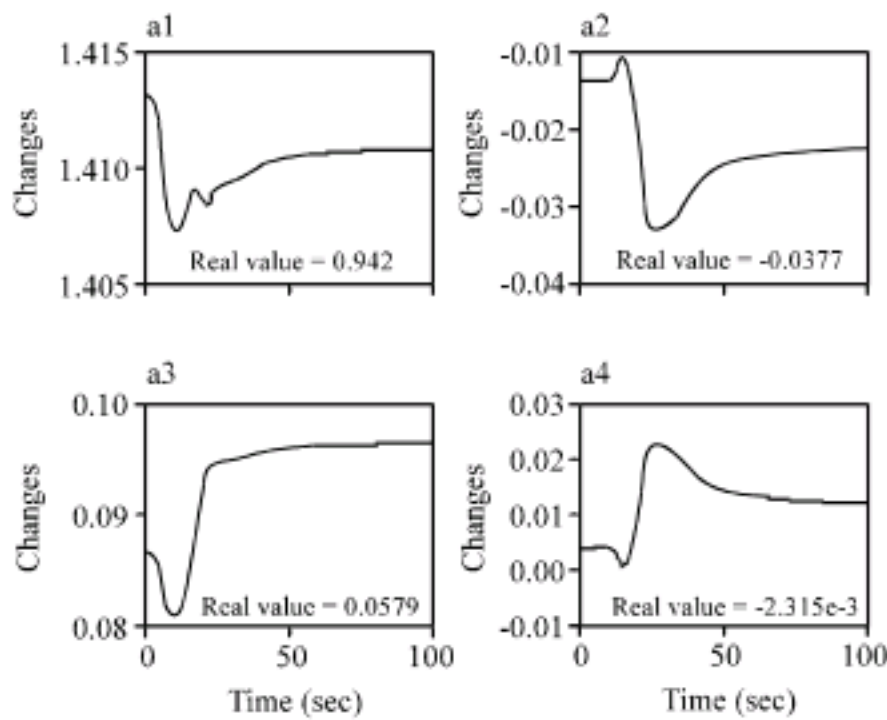


Fig. 12: Changes in the estimated parameters in case of changes in mass

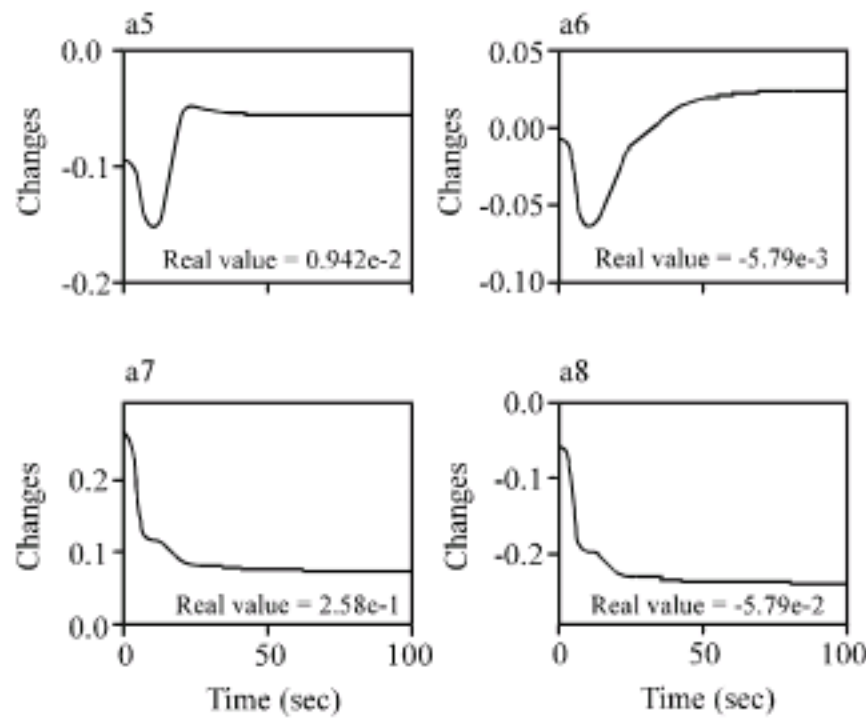


Fig. 13: Changes in the estimated parameters in case of changes in mass

can realize that the 40th second is the time that the mass stops changing and the curve has its peak. Figure 12 and 13 show the curves of changes in parameters in such case. In this case, the parameters do not converge to their actual values because the signal that is used for estimation of the parameters is not a PE signal.

Noise: Noise-robustness is an important issue in a control system because all sensors collect noise from the environment. On the other hand, noise exists in all environments. In the following First, the effects of noise are discussed and then perturbation in the output of the control input is investigated.

To investigate the effects of noise, the adaptive algorithm and its noise-robustness capability is discussed and if the system is robust to a large domain of noise, the proposed adaptive control algorithm should be corrected. To do so toward this, it is started with the small value of

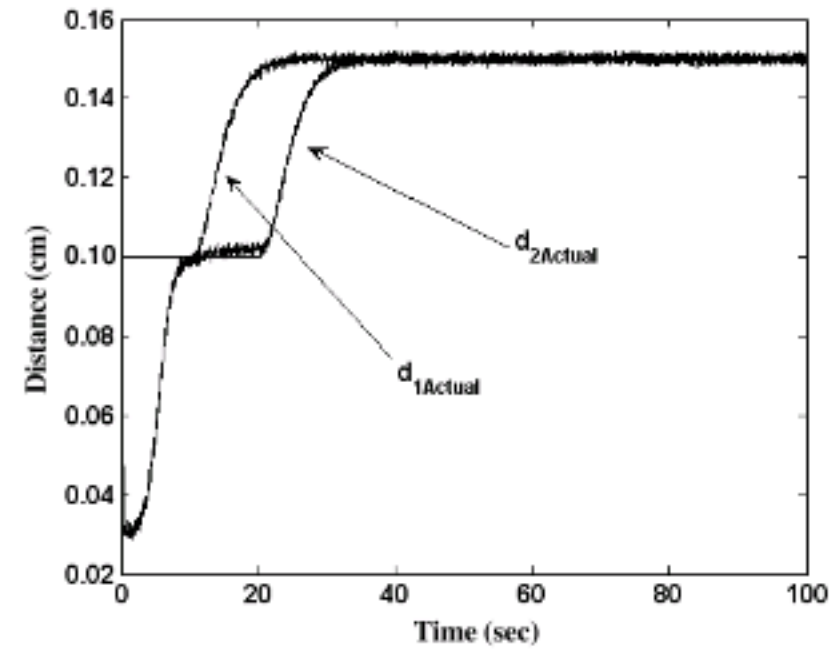


Fig. 14: The output of the system in presence of noise

$1e-5$ for the noise domain and gradually increase the noise domain. The output of the system for the following cases of measuring of the domain of the noise signals is shown in Fig. 14.

$$\begin{aligned}
 &\text{for } x_1 \ 1e-3 \\
 &\text{for } x_2 \ 1e-3 \\
 &\text{for } x_3 \ 1e-3 \\
 &\text{for } x_4 \ 1e-3 \\
 &\text{for } x_5 \ 1e-2 \\
 &\text{for } x_6 \ 1e-2
 \end{aligned} \tag{47}$$

As it can be seen in the Eq. 47, the noise domain for x_5 and x_6 is 10 times larger than that of other variables. Because these two variables represent electrical current which have a domain 10 to 20 times larger than other state variables. Considering the domain of the noise for the state variables can be translated to inaccurate measuring instruments of electrical current in comparison with the sensors of measuring the position and velocity. In other simulations these relations are preserved. Figure 14 shows that the proposed system is robust to the noise in Eq. 47.

The way in which the parameters change is shown in Fig. 14. In the next experiment, the domain of the noise is multiplied by 10 and the estimated parameters do not converge to the real values (Fig. 15, 16) because the signal that is used for the estimation of the parameters is not a PE signal. In such case, the system diverges in the 4th time step as shown in Fig. 17. To solve this problem, the adaptation rule is changed to what follows:

$$\dot{p} = \frac{p\xi\xi^T p}{1 + \xi^T p\xi} \tag{48a}$$

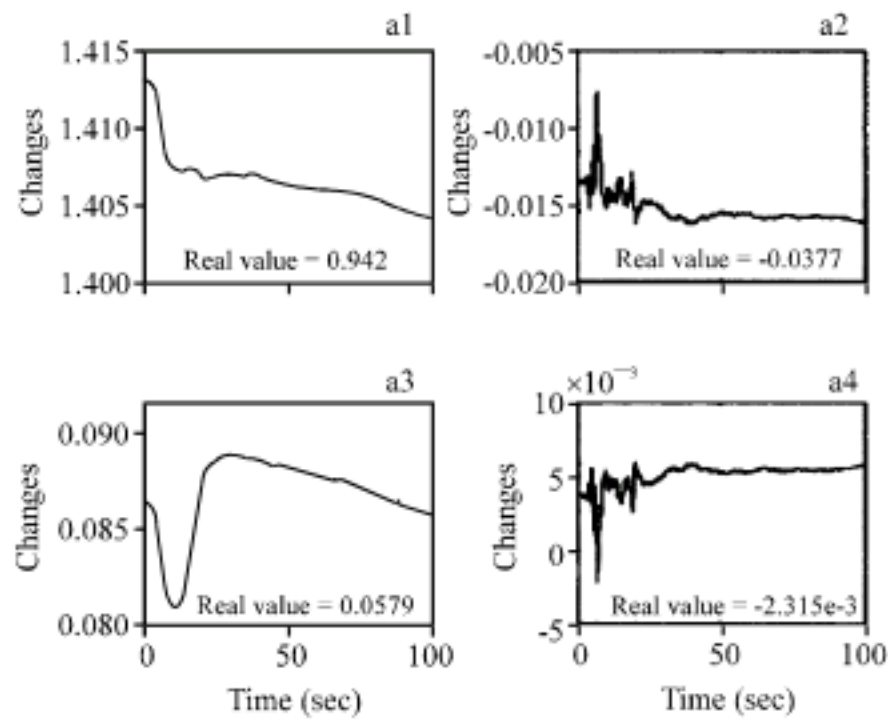


Fig. 15: The changes of the parameters

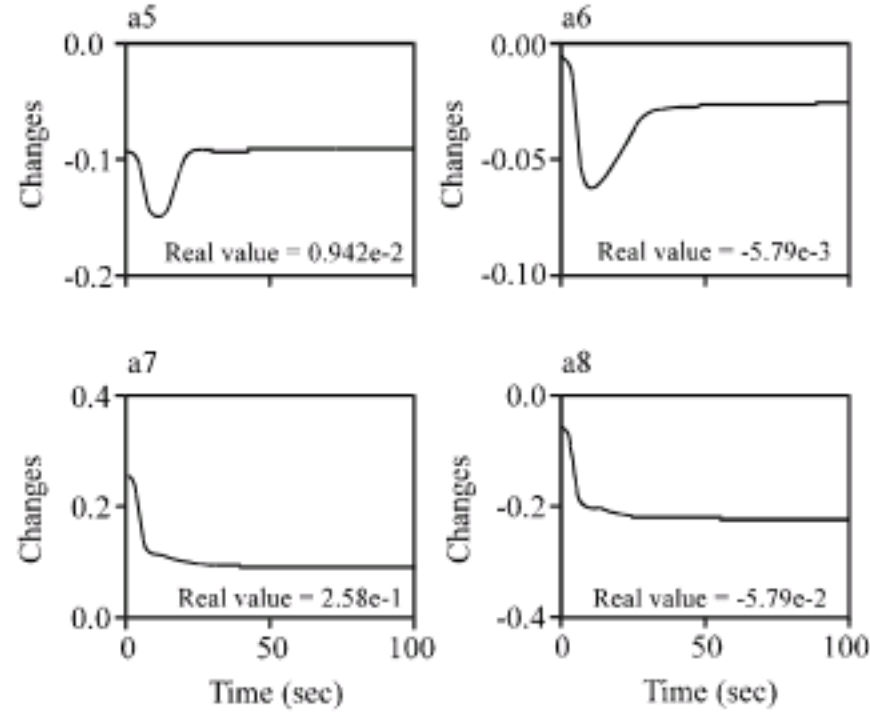


Fig. 16: The changes of the parameters

$$\dot{\theta}_e = \dot{\Phi} = \begin{cases} \frac{-p\xi e_1}{I + \text{norm}(\xi^T p \xi)} + \frac{p(w \times \text{norm}(e_1) \times \theta_e)}{I + \text{norm}(w \times p \times w)} & \text{for } \text{norm}(\dot{p}) > R_0 \\ 0 & \text{otherwise} \end{cases} \quad (48b)$$

As it is shown in the Eq. 48b, in order to implement the algorithm, estimation of the parameters is needed. In Eq. 48, w and R_0 are design parameters. In the simulation, these values are considered as follows:

$$\begin{aligned} w &= 50 \\ R_0 &= 10 \end{aligned} \quad (49)$$

Once again, the domain of noise in Eq. 47 is multiplied by 10. The output of the system is shown in Fig. 18. As shown in this figure, despite the presence of noise with large domain, the adaptive algorithm has a satisfying performance and the output of the system follows the reference value and its fluctuations. The proposed

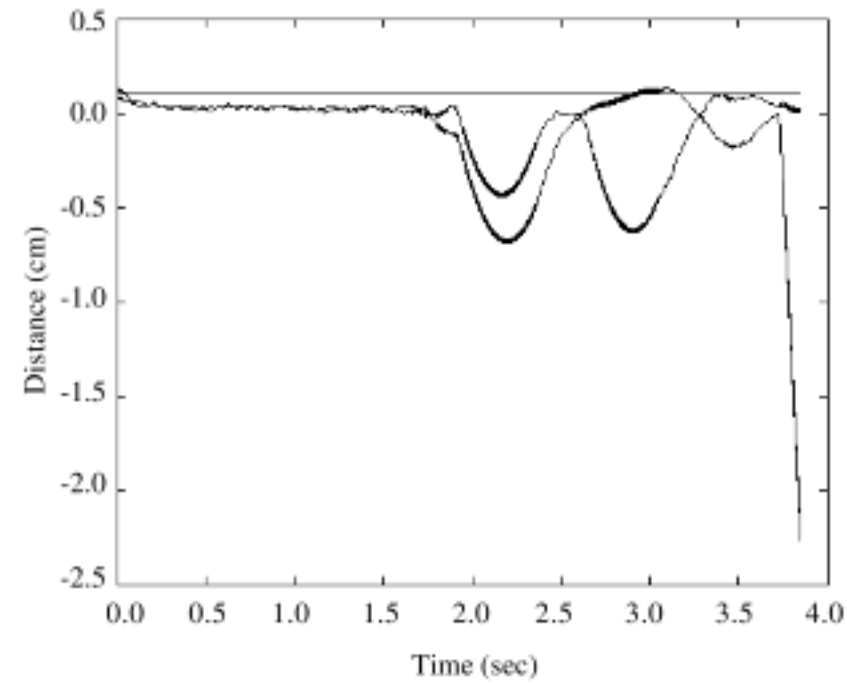


Fig. 17: The output of the proposed algorithm presence of noise

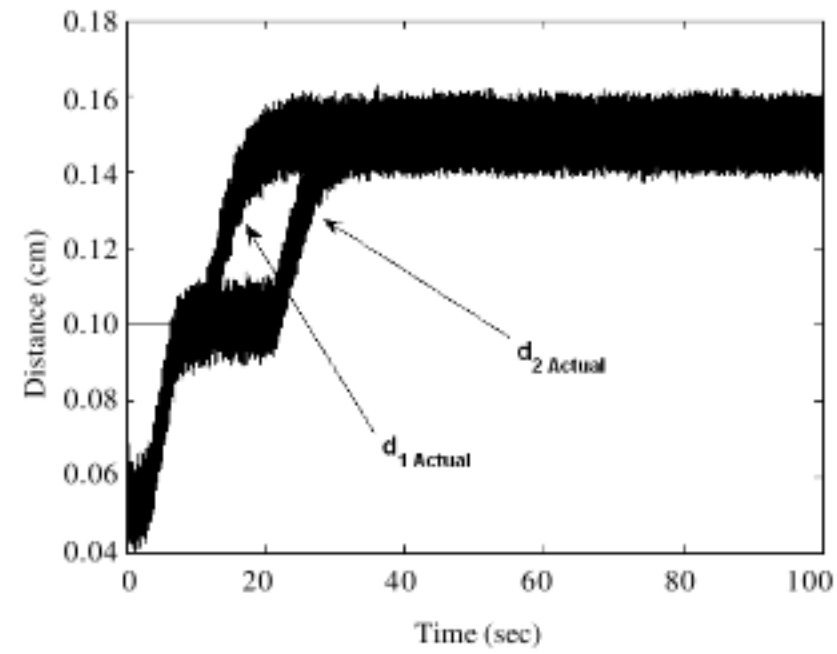


Fig. 18: The output of the system for the enhanced adaptive algorithm in presence of noise

algorithm here is the enhanced version of the algorithm for which the leakage and the dead zone is taken into account. The term $p(w \times \text{norm}(e_1) \times \theta_e) / I + \text{norm}(w \times p \times w)$ is related to the leakage and R_0 represents the dead zone. The term $\text{norm}(e_1)$ appears in the leakage term because the influence of this term decreases with the combinational error and the algorithm becomes more and more similar to the adaptive algorithm that is proposed in the past.

Figure 19 and 20 show the changes in the estimated parameters and Fig. 21 shows the norm fluctuations of \dot{p} . This value can be considered as a measure for the convergence of the parameters. In addition, this norm can be used to determine the dead zone.

Perturbation in the input: The simulation results indicate that perturbation in the input hardly affects the algorithm. Since, the control input of the system in absence of noise

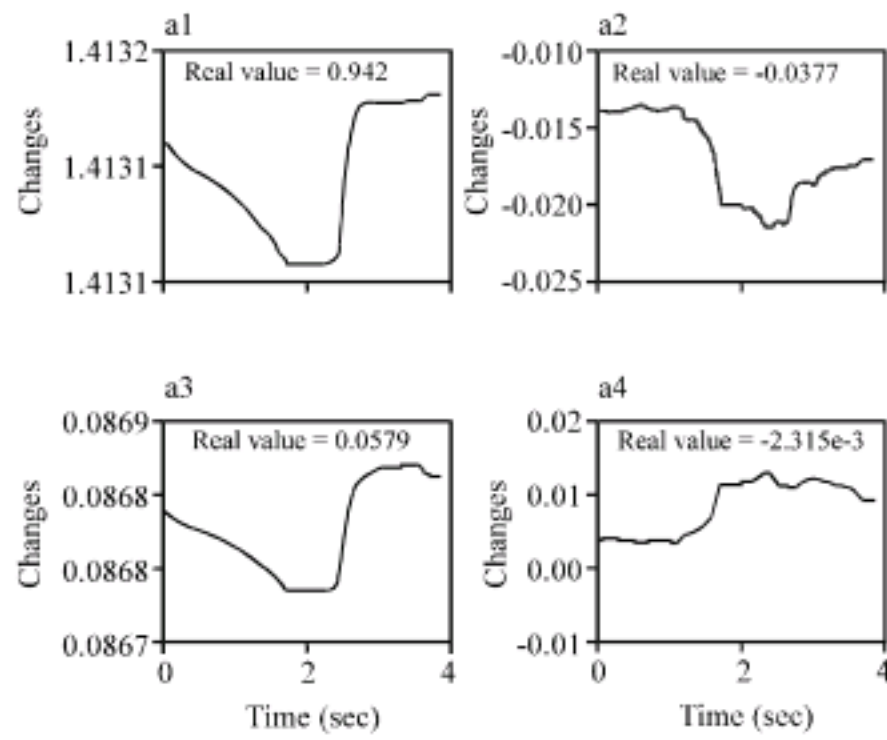


Fig. 19: The change in estimated parameters for the enhanced adaptive algorithm in presence of noise

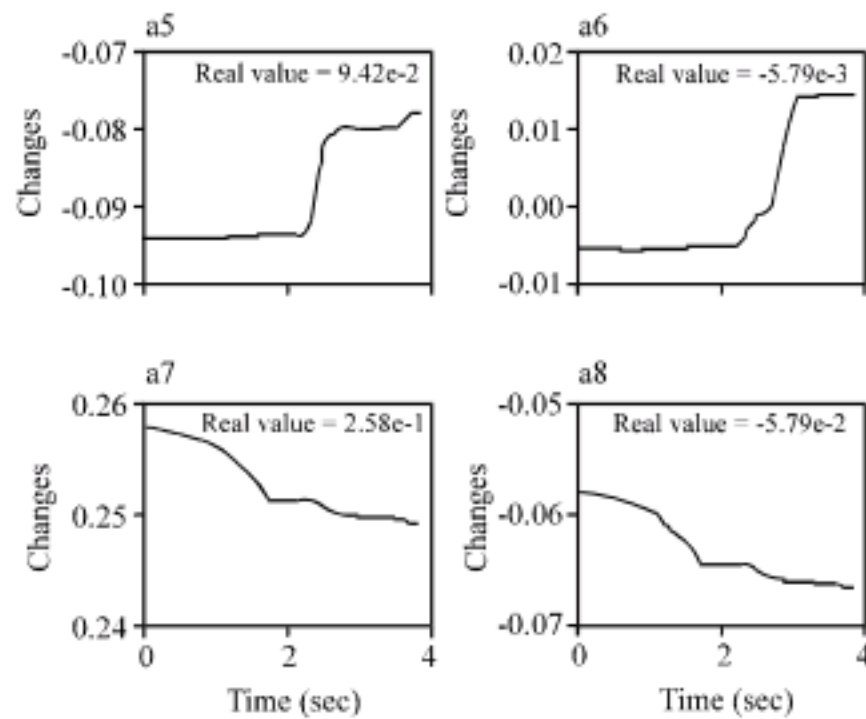


Fig. 20: The change in estimated parameters for the enhanced adaptive algorithm in presence of noise

and perturbation is about 50 volts. To show the satisfying performance of the proposed algorithm in the past in presence of perturbation and absence of noise, the perturbation domain is set to 20. As shown in Fig. 22, in this case, the system is capable of following the reference value satisfactorily. In Fig. 23, 24, the change in the estimated parameters is shown. Since noise avoidance cannot be done completely, the same perturbation is considered for the adaptive algorithm in absence of noise. The simulation results show that in such case, complete trajectory following is not possible but if perturbation is added to the system, complete following is reachable by fluctuating around the reference value.

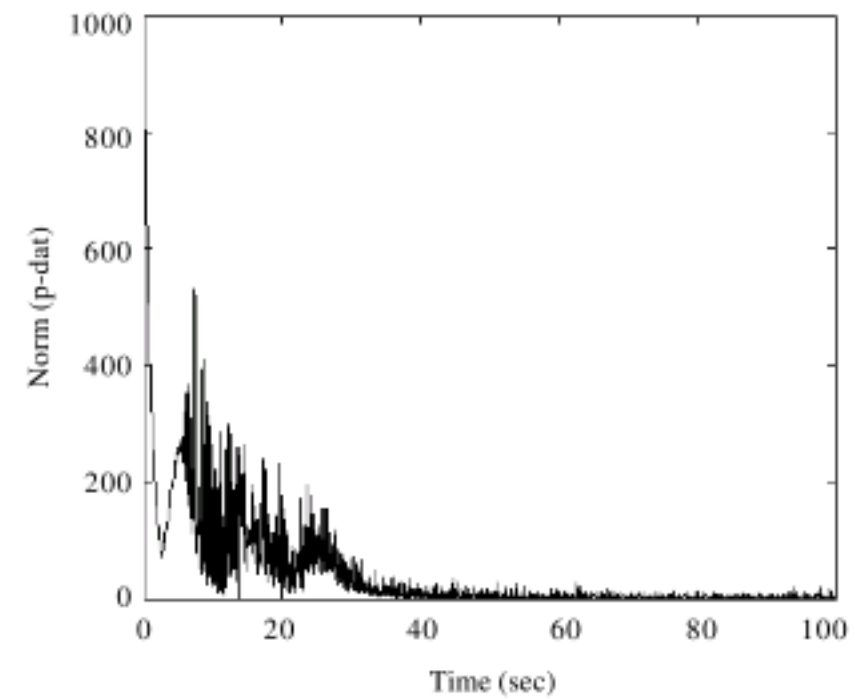


Fig. 21: The fluctuations of norm of \dot{p}

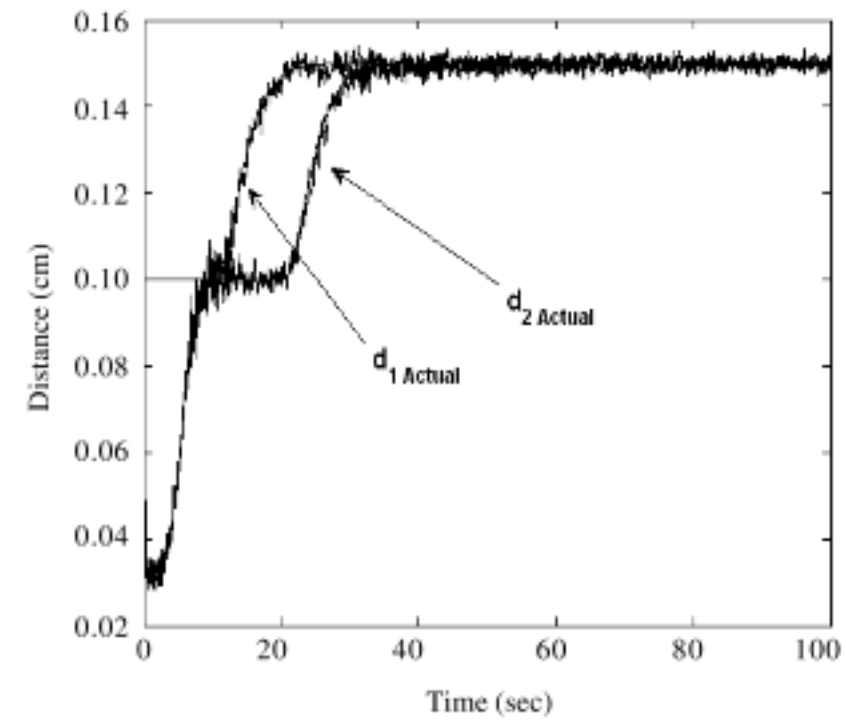


Fig. 22: The output of the control system by using the algorithm in presence of perturbation

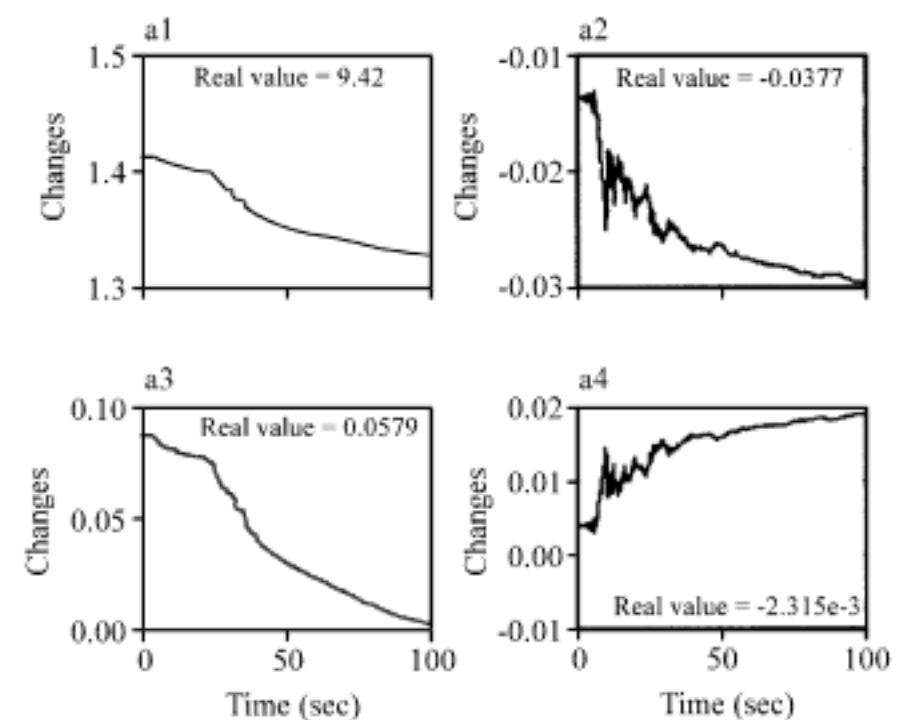


Fig. 23: The change in estimated parameters by using the algorithm in presence of perturbation

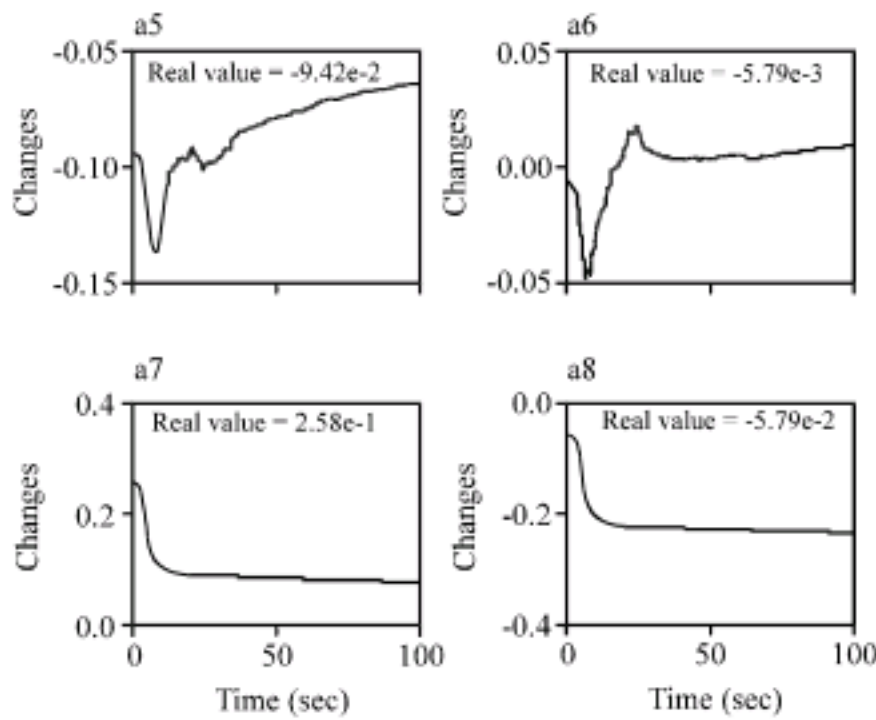


Fig. 24: The change in estimated parameters by using the algorithm in presence of perturbation

CONCLUSION

As mentioned earlier, this study is presented in order to improve the study of De-Sheng and Kun (2006) for overcoming the problems such as noise and disturbance, mass changes of the train and uncertainties of parameters which decrease the efficiency of their method. As the simulation shows the current proposed method will overcome all of these problems. In this study, an enhanced adaptation algorithm based on the normalized least square algorithm is implemented. As the simulation results show, the proposed algorithm has a satisfying performance in tracking in presence of unknown changes in the mass. The advantage of the proposed algorithm in comparison to non-linear controllers is that knowing the mass changes is not necessary. It is also noticeable that the initial values of the parameters cannot be set to zero because the parameters diverge time goes by due to the structure of the system. As shown, the system is sensitive to noise in measurement and perturbation in output shows less sensitivity to perturbation in the input. Generally, it was also shown that in the presence of input and output perturbation, the modified proposed algorithm ends to the satisfying results.

REFERENCES

Aliasghary, M., M. Teshnehlab, A. Jalilvand, M. Aliyari Shoorehdeli and M.A. Nekoui, 2008. Hybrid control of magnetic levitation system based-on new intelligent sliding mode control. *J. Applied Sci.*, 8: 2561-2568.

Bonivento C., L. Gentili and L. Marconi, 2005. Balanced robust regulation of a magnetic levitation system. *IEEE Trans. Control Syst. Technol.*, 13: 1036-1044.

Chen, M.Y., M.J. Wang and L.C. Fu, 2003. A novel dual-axis repulsive maglev guiding system with permanent magnet: Modeling and controller design. *IEEE/ASME Trans. Mechtrnacs*, 8: 77-86.

De-Queiroz M.S. and S. Pradhananga, 2007. Control of magnetic levitation systems with reduced steady-state power losses. *IEEE Trans. Control Syst. Technol.*, 15: 1096-1102.

De-Sheng L., L. Jie and Z. Kun, 2006. Design of nonlinear decoupling controller for double-electromagnet suspension system. *Acta Automatica Sinica*, 32: 321-328.

Fialho, I. and G.J. Balas, 2002. Road adaptive active suspension design using linear parameter-varying gain-scheduling. *IEEE Trans. Control Syst. Technol.*, 10: 43-54.

Hassanzadeh, I., S. Mobayen and G. Sedaghat, 2008. Design and implementation of a controller for magnetic levitation system using genetic algorithms. *J. Applied Sci.*, 8: 4644-4649.

Huang, S.J. and W.C. Lin, 2003. Adaptive fuzzy controller with sliding surface for vehicle suspension control. *IEEE Trans. Fuzzy Syst.*, 11: 550-559.

Khalil, H.K., 2002. *Nonlinear Systems*. 3rd Edn., Prentice-Hall Inc., Upper Saddle River, New Jersey, ISBN: 0-13-067389-7.

Li, Y.G. and W.S. Chang, 1999. Cascade control of an ems maglev vehicle's levitation control system. *Acta Automatica Sinica*, 25: 247-251.

Lin, F.J., H.J. Shieh, L.T. Teng and P.H. Shieh, 2005. Hybrid controller with recurrent neural network for magnetic levitation system. *IEEE Trans. Magnetics*, 41: 2260-2269.

Liu, D.S., J. Li and K. Zhang, 2005. The design of the nonlinear suspension controller for ems maglev train based on feedback linearization. *J. National Univ. Defense Technol.*, 27: 96-101.

Namerikawa, M.T. and M. Fujita, 2001. Uncertainty structure and μ -synthesis of a magnetic suspension system. *T. IEE Jap.*, 121-C: 1080-1087.

Peterson, K.S., J.W. Grizzle and A.G. Stefanopoulou, 2006. Nonlinear control for magnetic levitation of automotive engine valves. *IEEE Trans. Control Syst. Technol.*, 14: 346-354.

Slotine, J.J.E. and W. Li, 1991. *Applied Nonlinear Control*. 1st Edn., Prentice Hall, Englewood Cliffs, New Jersey, ISBN: 0-13-040890-5.

- Wai, R.J. and J.D. Lee, 2008a. Adaptive fuzzy-neural-network control for maglev transportation system. *IEEE Trans. Neural Networks*, 19: 54-70.
- Wai, R.J. and J.D. Lee, 2008b. Backstepping-based levitation control design for linear magnetic levitation rail system. *IET Control Theor. Appl.*, 2: 72-86.
- Yang, Z.J., K. Kunitoshi, S. Kanae and K. Wada, 2008. Adaptive robust output-feedback control of a magnetic levitation system by K-filter approach. *IEEE Trans. Ind. Elect.*, 55: 390-399.